

# Implementation of an Integrated Health Risk Assessment Coupled with Spatial Interpolation and Source Apportionment: A Case Study of Soil Heavy Metals, China

**Fangfang Miao**

North China Electric Power University

**Yimei Zhang** (✉ [mist1218@tom.com](mailto:mist1218@tom.com))

North China Electric Power University

**Yu Li**

North China Electric Power University

**Qinglu Fang**

North China Electric Power University

**Yinzhuang Zhou**

Capital Normal University

---

## Research Article

**Keywords:** Soil heavy metals, Spatial interpolation, Global data optimization, Quantitative source apportionment, Source-identified health risk

**Posted Date:** September 3rd, 2021

**DOI:** <https://doi.org/10.21203/rs.3.rs-850896/v1>

**License:**  This work is licensed under a Creative Commons Attribution 4.0 International License.

[Read Full License](#)

---

1 **Implementation of an integrated health risk assessment coupled with spatial**  
2 **interpolation and source apportionment: A case study of soil heavy metals, China**

3 Fangfang Miao<sup>a</sup>, Yimei Zhang<sup>a,b\*</sup>, Yu Li<sup>a</sup>, Qinglu Fang<sup>a</sup>, Yin Zhuang Zhou<sup>c,d</sup>

4 <sup>a</sup> MOE Key Laboratory of Resources and Environmental System Optimization, College of Environmental Science  
5 and Engineering, North China Electric Power University, Beijing, 102206, China

6 <sup>b</sup> Laboratory of Environmental Remediation and Functional Material, Suzhou Research Academy of North China  
7 Electric Power University, Suzhou, Jiangsu, 215213, China

8 <sup>c</sup> Key Laboratory for Northern Urban Agriculture of Ministry of Agriculture and Rural Affairs, College of Bioscience  
9 and Resources Environment, Beijing University of Agriculture, Beijing, 102206, China

10 <sup>d</sup> Department of Chemistry, Capital Normal University, Beijing 100048, PR China

11 E-mail: zhangym@ncepu.edu.cn; Fax:86-0512-67332655; Tel: 86-0512-67332668

12 Address: Suzhou Research Academy of North China Electric Power University, Suzhou, Jiangsu, 215123, P.R.China

13 **Abstract**

14 Soil heavy metal contaminated sites with multiple sources of pollution have caused worldwide public concern.  
15 However, the lack of correlation of risk assessment between source identification of heavy metal led to unclear  
16 direction of source governance. A methodology was established by combining source apportionment of human health  
17 risks with ecological enrichment to characterize source-identified risks of heavy metals based on Ordinary kriging  
18 interpolation. Principal component analysis (PCA) and positive matrix factorization (PMF) model were used to  
19 identify and classify potential sources of heavy metals synthetically. The integrated results were incorporated into the  
20 health risk model to evaluate potential non-carcinogenic and carcinogenic risk of soil heavy metals. A case study was  
21 conducted in Suzhou city of China. The results showed that concentrations of Cd and Hg were highly above the  
22 background values, accounting for percentages of 239.6% and 415.9% above background values, respectively. The  
23 source contributed human health risk index of As contributed 76.9% to non-carcinogenic risk by pollutant sources of

24 agriculture activities. The Non-cancer health risk index for children and adults was 1.08 and 1.00 respectively. The  
25 cancer health risk was  $3.67E-03$  for children and  $3.97E-04$  for adults. Cr originated from industry activities,  
26 accounting for 29.5% of total heavy metals, and constituted the largest carcinogenic impact on the population. This  
27 study provided a new insight for the treatment of multiple sources of soil heavy metal pollution and also some reference  
28 value for the improvement of the risk assessment system.

29 **Keywords:**

30 **Soil heavy metals; Spatial interpolation; Global data optimization; Quantitative source apportionment;**  
31 **Source-identified health risk**

32 **1. Introduction**

33 Soil was the most important natural resource of a country and the material basis of the environment where human  
34 beings live on (Liang et al., 2017; Järup, 2003). However, with the increasing agricultural production, industrial  
35 activities and human activities, great pressure was put on the soil quality continually, resulting in direct soil pollution,  
36 especially soil heavy metal pollution (Ihedioha et al., 2017; Salmani-Ghabeshi et al., 2016; Luo et al., 2011). The  
37 heavy metal pollutants in soil mainly include Hg, Cd, Pb, Cr, Cu, Ni, Co, Sn and the metal-like As. Distinct from other  
38 pollution, heavy metal pollution was not easy to be leached with water and decomposed by microorganism in soil  
39 (Xie et al., 2016; Papa et al., 2010). There were four main ways in which heavy metals entered the soil: atmospheric  
40 deposition (natural and man-made), fertilizers containing metal impurities, industrial emission, and irrigation of  
41 contaminated water (Luo et al., 2015; Liu et al., 2017). Afterwards heavy metals entered the food chain through  
42 accumulation in plants and have obvious biological enrichment, posing risks to the ecosystem and human health (Han  
43 et al., 2006; Kurt-Karakus, 2012). In addition, heavy metal was often tightly bound to soil solids, and even small  
44 increases in the current concentration of heavy metals can have potentially adverse effects on soil quality (Islam et  
45 al., 2017; Noll, 2002). Due to the increasingly serious soil pollution, it was important to predict the accumulation  
46 trend of heavy metals in soil and understand the risk level of heavy metal pollution (Teng et al., 2010). Therefore, it

47 was of far-reaching significance to effectively assess the pollution situation, including potential local ecological risks,  
48 identify potential pollution sources, so as to provide information for soil pollution control (CSC, 2016). So far, many  
49 research groups had worked on the investigation of soil pollution (Couto et al., 2018; Mendoza et al., 2017). However,  
50 most of these studies focus on agricultural pollution or water pollution, and there were comparatively few studies on  
51 the soil pollution of abandoned dye factory (Gholizadeh et al., 2019; Xiao et al., 2019; Mohammadi et al., 2020;).  
52 The soil environment of many factories in the whole country of China was not optimistic and was serious in some  
53 areas (Chen et al., 2015). To strengthen environmental management, a series of policies were implemented to focus  
54 on seriously polluted enterprises and force the closure of the small and heavily polluted factories. The pollution of  
55 some heavy metals in the soil left by such closed enterprises deserved our attention. The site of the original production  
56 enterprises in the process of development, especially dyeing factories, may be polluted by heavy metals (Mao et al.,  
57 2019). Pollutants often existed in waste water and waste residue which may leak through the staging point, migration  
58 of elution infiltration into the soil and rivers (Wcislo et al., 2016). Therefore, the original location and the  
59 surroundings may be polluted, leading great harm to the ecological environment and human health. So it was  
60 necessary to scrap the dye factory for soil pollution characteristics, ecology and human health risk assessment.  
61 Scholars at home and abroad had carried out extensive studies on soil pollution characteristics and human health risk  
62 assessment in the surrounding areas such as coal production, transportation and storage, as well as coal-fired power  
63 plants, but there were few reports on the investigation and assessment of soil pollution in abandoned dyestuff factories  
64 (Jia et al., 2015). Therefore, it was necessary to further study the soil pollution in the abandoned dye factory area in  
65 order to make better use of the site and provide reference for the site remediation in the next step.

66 To reduce the hazard of soil heavy metals, source apportionment can be an effective tool to quantify the pollution  
67 sources of heavy metals in polluted sites (Jiang et al., 2019; Guan et al., 2018). Even if there were some studies on  
68 the classification of pollution sources of soil heavy metals. Studies organically combined the contribution rate of  
69 source analysis with human health risk had also been reported, but few about systematic relevance between them

70 (Xiao et al., 2019). In order to better understand the pollution level of heavy metals in soil, spatial interpolation  
71 method was often used to obtain the concentration distribution of heavy metals in soil. In addition, enrichment factor  
72 (EF) was also calculated to obtain the ecological enrichment information of soil pollution (Tian et al., 2017; Nazzal  
73 et al., 2016). It was essential to find out further information about the characteristic distribution, pollution sources  
74 and environmental risks of heavy metals in polluted sites (Jiang et al., 2017; Niu et al., 2020). Identifying potential  
75 pollution sources of heavy metals was the basic premise for designing targeted pollution control measures. Although  
76 source apportionment and environmental risk assessment of heavy metal pollution had been carried out in many  
77 studies and the study of source-specific health risk and potential ecological risk based on the contribution rate of  
78 source analysis was also been reported (Peng et al., 2016). However, they mainly focused on the heavy metals from  
79 atmospheric and urban river-lake system (Tapia-Gatica et al., 2020; Li et al., 2020). Metal pollution from abandoned  
80 dye factories had been scarcely reported, let alone the overall impact of health risks on the study area. Positive matrix  
81 factorization (PMF) and Principal component analysis (PCA) was widely used for pollution source analysis in various  
82 media such as the atmosphere, hydrosphere and soil sphere (Liang et al., 2017a; Lang et al., 2015). It can be applied  
83 to apportion the potential sources of heavy metals (Norris et al., 2014). Compared with traditional multivariate  
84 statistical analysis methods, PMF was able to deal with the measurement uncertainty inherent in environmental data  
85 (Paatero and Tapper, 1994; Lv and Liu, 2019). Quantitative source analysis and its contribution research were helpful  
86 to identify the main pollution sources and quantified their contribution rate (Yang et al., 2019; Kumar et al., 2019). In  
87 addition, the city we studied, Suzhou, as a developed industrial area, the closure of polluting factories will inevitably  
88 led to the intensification of other human activities driven by the economy (Zhang et al., 2018). Therefore, there  
89 was the need to conduct the first detailed evaluation of the total effects of health risks on soil heavy metals associated  
90 with the areas related to a dye factory in the southeast of Suzhou by using multivariate statistical and spatial analysis  
91 methods.

92 This paper mainly dealt with: (i) the optimized spatial interpolation of heavy metal concentration to obtain global

93 data in the sampling sites with reference to the Soil Guide of China (National Environmental Protection Agency,  
94 1995);(ii) Multivariate statistics and spatial distribution of ecological enrichment for analyzing the ecological  
95 pollution levels; (iii) identification of potential sources of soil heavy metals pollution and quantification of the  
96 proportions of various sources through combination of PCA and PMF models; (iv) Calculation of source-contributed  
97 human health risk index; (v) total effects of health risks on soil heavy metals. This study can provide reference for  
98 soil remediation and protection design in the study area and also reference for policy formulation and protection  
99 research on soil heavy metal pollution in other areas.

## 100 **2. Materials and methods**

### 101 **2.1. Case study**

#### 102 **2.1.1. Study area and sampling**

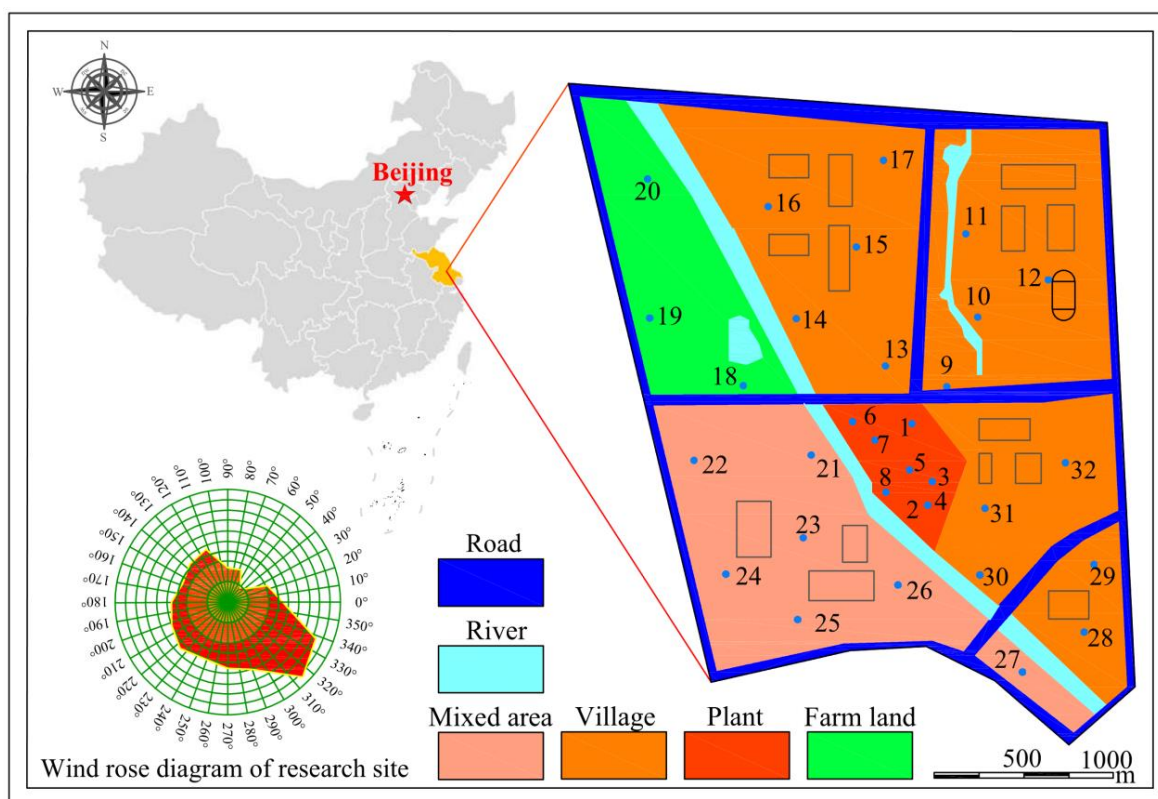
103 Suzhou was located in the middle of the Yangtze river delta, the southeast of Jiangsu province, located at 119°55'E  
104 to 121°20'E, 30°47'N to 32°02'N, east of Shanghai, south of zhejiang, west of taihu lake, north of the Yangtze river,  
105 the total area of 8657.32 square kilometers. The city was low-lying and flat, with many rivers and lakes. Most of the  
106 water surface of taihu lake were in suzhou. Rivers, lakes and beaches accounted for 36.6% of the city's land area.  
107 Suzhou was a subtropical monsoon maritime climate, with an average temperature of 17.8°C and precipitation of  
108 1369.2mm in 2018. The prevailing wind direction was southeast wind all year along, with four distinct seasons, mild  
109 climate, abundant rainfall, fertile land, rich natural conditions and so on. In the shallow layer, the clay soil with slight  
110 deformation and high strength was mainly grey, with compact texture.

#### 111 **2.1.2. Sample collection and chemical analysis**

112 According to the land use pattern, topographic features and perennial wind direction in the study area, 30 composite  
113 topsoil samples in the 0-7cm layer were randomly collected for measurement in Suzhou in October 2019 and the  
114 exact location of each point was recorded in **Fig .1**. The soil samples were taken back to the laboratory and naturally  
115 dried and ground crushing, first through a 20 mesh sieve for pH analysis, then used for the determination of physical

116 and chemical properties (Pal et al., 2019). The processed soil samples were dissolved in the mixture acid solution  
117 ( $\text{HNO}_3\text{-HF-HClO}_4$ ) at a high temperature of 210°C for 4h (Bryanin et al., 2019). Soil pH was determined with a ratio  
118 of 2:5 (w/v) soil/water mixture using a pH meter (Cheng et al. 2018). The soil organic matter (SOM) content was  
119 determined by the chromic acid titration method. The content of heavy metals As, Cd, Cr, Zn and Pb in soil samples  
120 were determined by Inductively Coupled Plasma-Mass Spectrometry (ICP-MS, PerkinElmer ELAN 9000).  
121 Atomic fluorescence photometer (AFS-230E) was used to analyze the content of Hg. Each batch of samples was  
122 evaluated by reagent blanks to reduce errors for quality assurance (Jiang et al., 2019).

123 To ensure the quality of analysis, several quality assurance and control methods were conducted as the following  
124 standard operating procedures. Blank reagents, duplicate samples and soil standard reference samples (GBW07401-  
125 07408, Beijing; National Center for Standard Materials of China) were operated in the Analytical and Testing Center  
126 of Suzhou research academy of North China Electric Power University. Chemical reagents are guaranteed reagents.  
127 The logarithmic deviation of the system was within the range of  $\pm 0.045$  (Zhang et al., 2017), and the relative  
128 percentage difference between duplicate samples was within the range of  $\pm 7.50\%$  (Han et al., 2006). Therefore, the  
129 precision and bias of the analysis were generally below 5%.



130  
131 **Fig. 1.** Sampling sites of soil heavy metals in the study area.

132 **2.1.3. Statistical analysis**

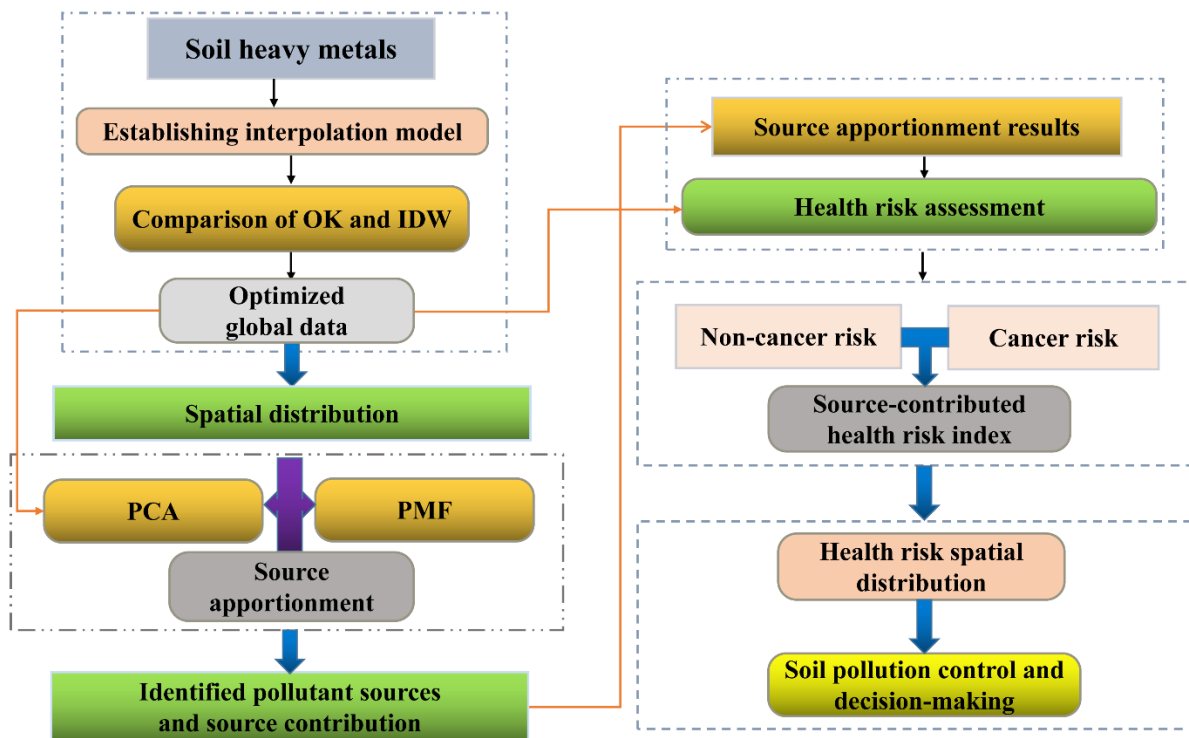
133 Microsoft Excel (version 2010, USA) was used for calculations. The spatial distribution of soil heavy metals was  
 134 mapped by the Surfer v.12.0 (Golden Software Inc., CO, USA) and ArcGIS 10.7 software. SPSS Statistics 25 (IBM  
 135 Inc., CO,USA) was used to conduct the analyses and to obtain the relevant parameters. The data underwent by EPA-  
 136 PMF 5.0 to assess the sources of soil heavy metals with a 95% confidence interval (significance  $p < 0.05$ ). Crystal  
 137 Ball Software (Version 2000, Decisioning, Denver, CO, USA) was employed for uncertainty analysis.

138 **2.2. Overview of the framework**

139 The city of Suzhou studied in this paper has a thriving ecotourism industry and there are abandoned industrial  
 140 polluted sites that have not been treated. Therefore, it is necessary to pay attention to the environmental health risks  
 141 in this region. The objective of this study is to conduct a combination of source analysis and health risk assessment  
 142 methodology to characterize the soil heavy metal pollution levels of the sources and source-specific human health  
 143 risk. The integrated framework of the method combined source apportionment and source-specific human health risk

144 assessment was shown in **Fig. 2**.

145 Firstly, the pollution sources is determined qualitatively by PCA analysis, and then the PMF source apportionment  
146 is carried out according to the obtained results to accurately define the types of sources and the distribution rate of  
147 pollution sources, which complement each other. Secondly, the spatial distribution of heavy metals in contaminated  
148 sites were studied by spatial interpolation based on the comparison of Ordinary kriging and inverse distance weighted.  
149 Besides, the contribution rate of pollution sources was used for risk sharing and the assessment results were  
150 incorporated into the health risk assessment model to identify heavy metal from identified sources. Thirdly, toxic  
151 metal with a large contribution from pollution sources and high risk level was screened out and the correlation and  
152 total effects of health risks have also been analyzed. Finally, we identify which sources of contamination need  
153 attention and which toxic metals need to be prioritized for removal or reduction of toxic emissions. Based on the  
154 above information, targeted risk reduction strategies can be developed. It provided a theoretical basis for the  
155 government to control heavy metal pollution scientifically (Huang et al., 2006; Luo et al., 2011).



156  
157 **Fig. 2.** Frameworks of the methodology for soil heavy metals.

### 158 **2.3. Optimization of spatial interpolation for global data of heavy metals**

159 **Step 1: Ordinary kriging (OK)**

160 Ordinary kriging was a type of kriging interpolation, which assumed that the property values were spatially  
161 stationary. OK interpolation routinely applied the weighted values of the attributes of known points as a predictor of  
162 the attributes of unknown points, which was mainly used to interpolate the parameters of un-sampled locations. The  
163 concentrations of soil heavy metals of the unknown point (x) was defined in **Eq. (1)**.

$$C_{(x)}^t = \sum_{i=1}^n \lambda_i C_{(x_i)}^t \quad (1)$$

164 where, the  $C_{(x)}^t$  was predicted concentration of soil heavy metals  $t$  ( $t = (\text{As, Cd, Cr, Hg, Pb and Zn})$  at unknown site  
165 of  $x$ ;  $C_{(x_i)}^t$  was the content of metal  $t$  at point  $x_i$  ( $i=1, 2, \dots, i, \dots, j, \dots, n$ ); was the concentration at the sampling point  $x_i$ ;  
166  $\lambda_i$  was the weight coefficient, which would be calculated by **Eq. (2)**.

$$\begin{cases} \sum_{i=1}^n \sum_{j=1}^n \lambda_i \lambda_j \gamma(x_i, x_j) + \mu = \gamma(x_i, x) \\ \sum_{i=1}^n \lambda_i = 1 \end{cases} \quad (2)$$

167 where, the  $x_j$  was another known point;  $\mu$  was the lagrangian constant;  $\gamma(x_i, x_j)$  was the semi-variogram function and  
168 could be obtained by **Eq. (3)**.

$$\gamma(h) = 1/2 E [C_{(x)}^k - C_{(x+h)}^k]^2 \quad (3)$$

169 Where,  $E$  was the number of sample pairs at a separation vector  $h$ .

170 **Step 2: Inverse distance weighted (IDW)**

171 The IDW method has a wide range of applications in the field of geology, which can be simplified as the estimation  
172 process of calculating the spatial variables of the concentration of heavy metals at unmeasured locations by observing  
173 a large number of measured samples in the space close to the target location.

174 Compared with alternative interpolation methods, IDW will comprehensively analyze the acute values (outliers)  
175 within the data set and predict the values of unknown areas (Goix et al., 2013). In general, the more similar the soil  
176 characteristics between the adjacent and unknown locations, the better the prediction results (Zhou and Sha, 2013).

177 The concentration of soil heavy metal  $C_{(x)}^k$  at the unknown point could be calculated by **Eq. (4)**.

$$C_x^k = \frac{\sum_{i=1}^n \frac{C_i^k}{D_i}}{\sum_{i=1}^n \frac{1}{D_i}} \quad (4)$$

178 Where,  $D_i$  ( $i=1, 2, \dots, n$ ) was the horizontal distance between interpolation point and reference point.

### 179 **Step 3: Verification method**

180 The accuracy of spatial interpolation methodology was verified by cross-validation model. The accuracy of both  
 181 Ok and IDW interpolation methods was evaluated by examination of the errors of observed value ( $OV$ ) and the  
 182 predicted value ( $PV$ ). The slope and determination coefficient ( $R^2$ ) of fitting line between the  $PV$  and the  $OV$   
 183 approaching to 1 indicated that the method would be more accurate.

## 184 **2.4. Mathematical models for source apportionment**

185 The PCA model was utilised to identify the sources of soil heavy metal pollution qualitatively first, and then the  
 186 PMF model was adopted for quantitative analysis to characterise the contribution of each source to soil heavy metal  
 187 pollution. A combined analysis was eventually undertaken based on the types of pollution sources obtained from the  
 188 two to accurately obtain the pollution sources and source contribution rates. The PCA/PMF model in combinatorial  
 189 form can effectively validate the two with each other to obtain a thorough and comprehensive assessment.

### 190 **2.4.1. Principal component analysis**

191 Principal Component Analysis (PCA) was a statistical method that simplified the data structure primarily by  
 192 dimensionality reduction, converting multiple variables into a small number of variables. PCA model could remodel  
 193 the initial data into a collection of linearly freelance representations of every dimension through linear transformation,  
 194 which can be used to extract the main feature components of data and was usually used for spatiality reduction of  
 195 high-dimensional data. The application of PCA in environmental science has been relatively mature, which can  
 196 effectively analyze the potential pollution sources and spatial distribution of heavy metals in soil (Xiao-Bo et al.,  
 197 2009). PCA was often used to identificate the natural and anthropogenic sources of heavy metals by means of using  
 198 chemical element principal factor loading (Cai et al., 2018; Hani and Pazira, 2011; Li et al., 2015).

### 199 **2.4.2. Positive matrix factorization**

200 The positive matrix factorization (PMF) method was one of the source analytical methods recommended by the  
 201 U.S. Environmental Protection Agency (Paatero et al., 2010). PMF was a factor analysis method based on the least  
 202 square method, which decomposed the matrix without negative constraints and can be optimized by means of  
 203 standard deviation of data (Chen et al., 2011). It did not rely on the chemical composition spectrum analysis of  
 204 pollution sources, but took the data sets of multiple soil samples and heavy metal elements as a matrix, and then  
 205 decomposed the matrix into the contribution rate matrix and the source composition spectrum matrix (Dong et al.,  
 206 2018; Franco et al., 2009). Through non negative constraint factor analysis and iterative calculation with the least  
 207 square method, the objective function was minimized to solve chemical mass balance between the measured heavy  
 208 metal concentration and pollution source (Guan et al., 2018). Compared with the traditional factor analysis method  
 209 (such as FA-MLR), the PMF method could avoid the negative value in the result of matrix decomposition, so that the  
 210 obtained source component spectrum and source contribution rate can be explained and had clear physical  
 211 significance (Lv et al., 2019). In addition, the PMF used error estimates for each individual data point in order to  
 212 cope with missing and inaccurate data more reasonably (Mamut et al., 2017). The data entered into the program  
 213 include concentrations and equation-based uncertainties (Jing et al., 2014).

214 The PMF had a unique advantage because it could be used without source components as input. It was also applied  
 215 to environmental data processing because it contained variable uncertainties associated with environmental sample  
 216 measurements and forced all values to be non-negative (Xue et al., 2014). Compared with the traditional source  
 217 apportionment methods, PMF was used to analyze pollution sources of heavy metals by weighing all data to analyze  
 218 the contribution rate of target variables (Tian et al., 2018). The method based on matrix equation was as follows:

$$C_{ik} = \sum_1^p g_{ip} f_{pk} + e_{ik} \quad (5)$$

$$Q = \sum_1^i \sum_1^k (e_{ik}/u_{ik})^2 \quad (6)$$

219 Where, the  $C_{ik}$  was the concentration of the  $k_{th}$  for soil heavy metals at the  $i_{th}$  sample;  $g_{ip}$  was the contribution of  
 220 the  $p_{th}$  source to the  $i_{th}$  sample;  $f_{pk}$  was the concentration of the  $k_{th}$  for soil heavy metals in the  $p_{th}$  source;  $e_{ik}$  was the

221 deviation of the  $k_{th}$  for soil heavy metals at the  $i_{th}$  sample;  $Q$  was the objective function;  $u_{ik}$  was the uncertainty of the  
 222  $k_{th}$  for soil heavy metals at the  $i_{th}$  sample.

223 The contribution rate of source  $m$  was obtained by Eq. (7).

$$g\% = (A_m / \sum_{m=1}^p A_m) \times 100\% \quad (7)$$

224 Where, the  $A_m$  referred to the regression coefficient for  $p_{th}$  source (Liu et al.,2018; Larsen and Baker, 2003).

## 225 2.5. Health risk assessment based on source-oriented model

226 Exposure to heavy metals may cause potential adverse effects on human health due to heavy metal toxicity.

227 Therefore, certain risk assessment model was developed by the USPEA and used frequently for the risk assessment.

228 There were three exposure routes contributed to the average daily dose (**ADD**) via ingestion, inhalation and dermal

229 contact. Non-carcinogenic hazards for heavy metals and the three exposure routes were calculated by the hazard

230 quotient (**HQ**) for two groups mainly including children and adults.

$$ADD_{ing} = C \times IngR \times EF \times ED / (BW \times AT) \times 10^{-6} \quad (9)$$

$$ADD_{inh} = C \times InhR \times EF \times ED / (PEF \times BW \times AT) \quad (10)$$

$$ADD_{dermat} = C \times SL \times SA \times ABS \times EF \times ED / (BW \times AT) \times 10^{-6} \quad (11)$$

$$HI = \sum_{i=1}^3 HQ = \sum_{i=1}^3 ADD_i / RfD_i \quad (12)$$

$$THI = \sum HI \quad (13)$$

$$CR_{sc}^i = ADD_i \times SF_i \quad (14)$$

231  $i$  represented each different exposure pathways of heavy metal entering the human body. **RfD** was the reference

232 dose (mg/kg-d) and parameters of detailed description of **RfD** were shown in **Table S1**; The hazard index (**HI**) is the

233 sum of **HQs** (Eq. (12)). The total hazard index (**THI**) is the sum of **HI** (Eq. (13)).  $CR_{sc}^i$  represented the carcinogenic

234 risk index of evaluating carcinogenic hazards of heavy metals (Zhang et al., 2018b). The other parameters were

235 provided by supplementary material in **Table S2**.

236 To better clarify the impact of pollution sources of heavy metals on human health, quantitative source

237 apportionment was combined with health risk assessment. Quantitative evaluation of *HI* and *THI* contributed from  
 238 each source were calculated by Eq. (15) to (17).

$$HI^k = HQ_{ing}^k + HQ_{inh}^k + HQ_{der}^k \quad (15)$$

$$HI_{sc}^{k,p} = HI^k \times g_p^k \quad (16)$$

$$THI_{sc}^{k,p} = \sum_1^k HI_{sc}^{k,p} \quad (17)$$

239 Where  $HI_{sc}^{k,p}$  was the source contributed hazard index of the  $k_{th}$  for soil heavy metals in the  $p_{th}$  source;  $THI_{sc}^{k,p}$  was  
 240 the total source contributed hazard index of soil heavy metals in the  $p_{th}$  source.

241 Carcinogenic risk (*CR*) for adults and children was evaluated to assess carcinogenic health effects on humans.  
 242 When *CR* and *TCR* greater than  $1 \times 10^{-4}$  were considered as unacceptable, while *CR* and *TCR* lower than  $1 \times 10^{-6}$  was  
 243 considered as no significant carcinogenic effects on humans.

$$TCR^k = CR_{ing}^k + CR_{inh}^k + CR_{der}^k \quad (18)$$

$$CR_{sc}^{k,p} = CR^k \times g_p^k \quad (19)$$

$$TCR_{sc}^{k,p} = \sum_1^k CR_{sc}^{k,p} \quad (20)$$

244 Where  $CR_{sc}^{k,p}$  was the source contributed carcinogenic risk of the  $k_{th}$  for soil heavy metals in the  $p_{th}$  source;  $TCR_{sc}^{k,p}$   
 245 was the total source contributed carcinogenic risk of all soil heavy metals in the  $p_{th}$  source.

246 Combined with quantitative source apportionment and risk assessment, the source-contributed health risk was  
 247 calculated. Human health risks of the pollution sources corresponding to soil heavy metals would be clearly displayed,  
 248 which was mainly to assess the hazards to human health of each specific source of pollution. The source-contributed  
 249 health risk was calculated by Eq. (21) to (22).

$$SCHI = HI_{sc}^{k,p} g\% \quad (21)$$

$$SCCR = CR_{sc}^{k,p} g\% \quad (22)$$

250 Where, the *SCHI* and *SCCR* represented the source-contributed non-carcinogenic and carcinogenic risk index of  
 251 each sources, respectively.

### 252 3. Results and discussion

#### 253 3.1. Description and optimized spatial interpolation of soil heavy metals

254 The pH value of the soil detected from the site studied was ranged from 7.03 to 7.57, the average value of which  
255 was 7.24. The summary statistics of heavy metals in soil from the site were presented in **Table 1**. The mean  
256 concentrations of different heavy metals decreased following the order: Cr > Zn > Pb > As > Cd > Hg. Compared  
257 with the background value, the mean concentrations of Cd, Hg and As were relatively higher than the background  
258 values (**BV**), accounting for percentages of 415.9%, 239.6% and 77.05% above **BV**, respectively. Additionally, the  
259 highest coefficient of variation (**CV**) of heavy metal turned out to be Hg followed by As and Zn, which indicated that  
260 the extensive variation may be affected by multiple factors, especially the anthropogenic activities (Fu et al., 2014).  
261 Furthermore, the concentrations of heavy metals (Cr, Pb and Zn) were close to the background values and the **CV** of  
262 them were lower than 50%, indicating moderate variability in the study area.

263 **Table 1**

264 Summary statistics for heavy metal concentrations (mg kg<sup>-1</sup>) in soils.

Element	Pb	Hg	Cr	Cd	As	Zn
Min	5.46	0.02	7.10	0.81	2.08	6.95
Max	81.57	1.51	80.59	28.95	56.88	84.32
Mean	28.42	0.18	71.03	0.65	17.75	69.45
Median	24.71	0.13	71.12	0.56	14.40	70.43
Variance	145.04	0.033	0.073	16.51	124.33	78.97
SD	12.04	0.18	0.27	4.06	11.15	65.63
CV	0.32	1	0.26	0.39	0.63	0.49
BV <sup>a</sup>	26.20	0.053	77.80	0.126	10.0	62.60
AV <sup>b</sup>	27.0	0.071	61.0	0.097	11.0	74.00
Chinese soil criteria <sup>c</sup>	250	2.5	150	0.3	30	200
Percent	8.50%	239.6%	0	415.9%	77.05%	10.94%

265 Note: GM- geometric mean; SD- standard deviation; CV- coefficient of variation; Percent- percentage above BV;

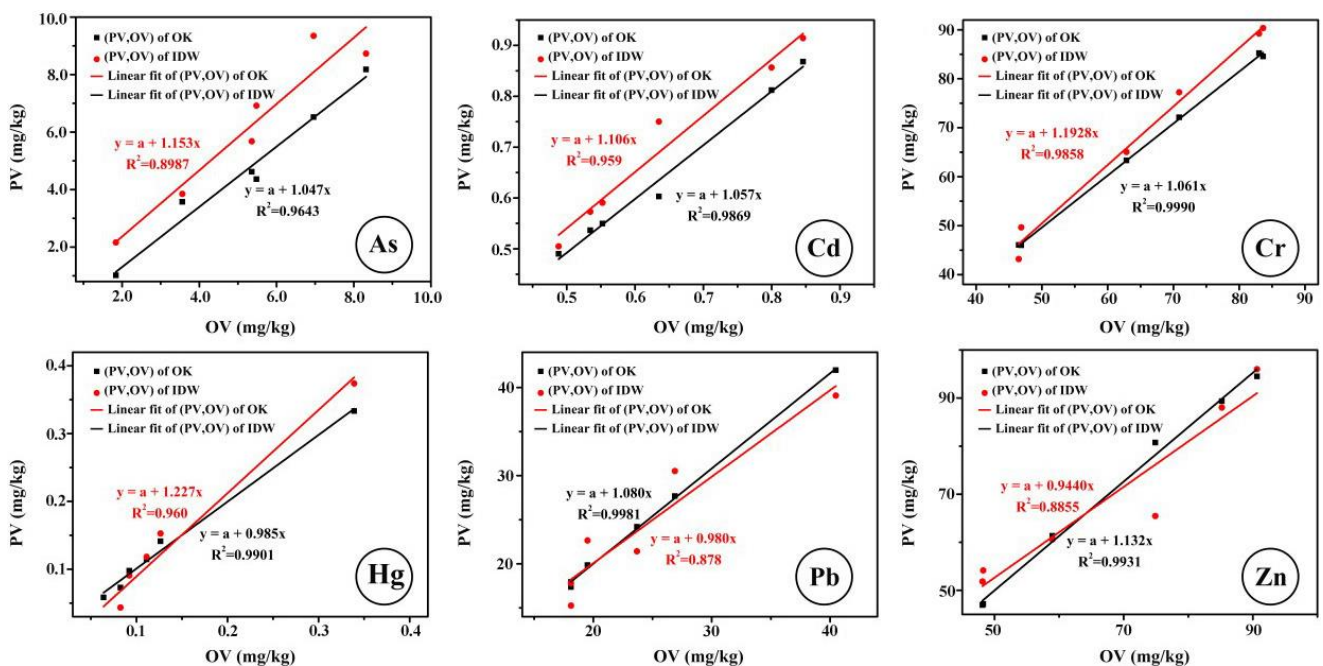
266 <sup>a</sup> BV-Background value of Jiangsu (Ma et al., 2015);

267 <sup>b</sup> AV-Average value of China (Wang et al. 2019a);

268 <sup>c</sup> Chinese soil criteria (CNEPA (1995)).

269 Trend analysis was performed according to the correlation coefficient between observed values (**OV**) and predicted  
270 value (**PV**) (**R**: square root of **R**<sup>2</sup>) to test the accuracy of the prediction method on the spatial distribution. Scatter  
271 trend analysis of soil heavy metals for **OV** and **PV** could convey a linear relationship with high **R**<sup>2</sup> values (0.85<**R**<sup>2</sup><1).

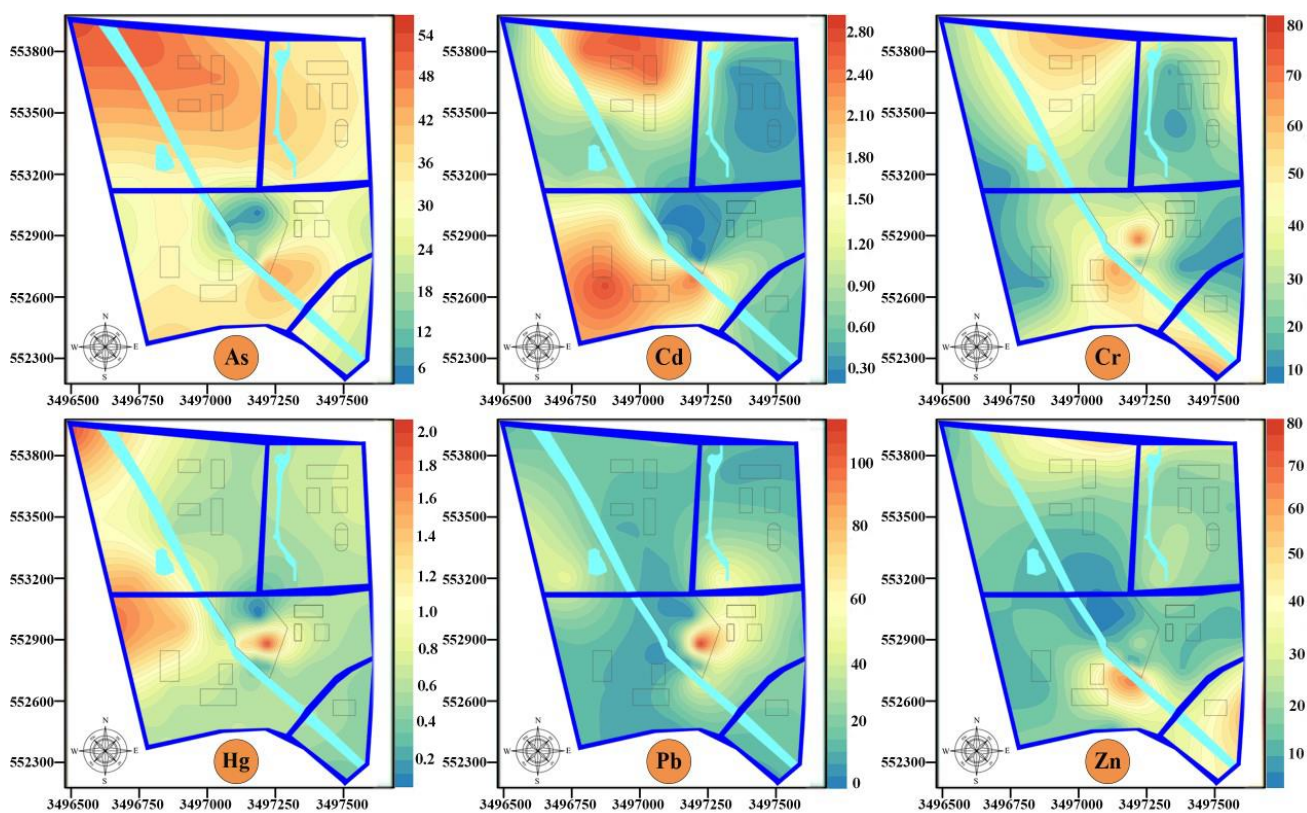
272  $R^2$  can fit the correlation between the simulated concentration and the observed concentration of soil heavy metals in  
 273 the spatial interpolation models (Islam et al., 2018). The results shown in Fig. 3 indicated that it was more reliable to  
 274 estimate the spatial distribution for the geological data collected. The Results demonstrated that the *PV* and *OV* values  
 275 were more close in the linear fit of heavy metals extracted by the *OK* method. Therefore, *OK* can provide a more  
 276 accurate prediction of the spatial distribution characteristics of heavy metals than *IDW*. *OK* allowed for the spatial  
 277 correlation of regional variables and the introduced variance function expressions to obtain globally optimal  
 278 interpolation data (Shahbeik et al., 2014). The introduced variance function can reduce the error in the spatial  
 279 interpolation results of heavy metals. Therefore, *OK* was more appropriate for the spatial distribution of the heavy  
 280 metals characterised in this study.



281  
 282 Fig. 3. Liner fitting for the predicted and observed values of soil heavy metals by *OK* and *IDW*.

283 Hence, the spatial distribution of the concentrations of heavy metals in the study area was depicted by means of  
 284 *OK* interpolation technique. As it can be seen from Fig. 4, the highly concentrated areas of spatial distribution of Cd  
 285 were mainly in the north and south-west of the study area. The concentrations of Pb and Zn had a similar tendency  
 286 for higher enrichment of the elements, mainly in the northwestern and southeastern part of the study area, which were

287 concentrated near the traffic roads. Meanwhile, the average concentrations of Zn and Pb were slightly higher than the  
288 background values for Jiangsu Province, mainly due to the proximity of this area to the northern part of the traffic  
289 roads in the study area, which could lead to higher levels of Zn and Pb when traffic flows increased. Areas of higher  
290 concentrations of Hg were present to the west and center of the dyeing plant. High concentrations of Cr were  
291 concentrated near the dye factory area and were close to background values. In addition, high concentrations of As  
292 were present around the north-western part of the study area, where agricultural land was located, particularly the  
293 overuse of fertilisers may lead to the accumulation of As.



294

295

Fig. 4. Spatial distributions of soil heavy metals in the study area using the interpolation model of *OK*.

## 296 3.2. Quantitative source apportionment in the study area

### 297 3.2.1. Pollution sources identification

298 The factor loading results by PCA for concentrations of soil heavy metals were showed in Fig. 5a. As shown in  
299 the figure, four principal components were extracted to reflect the relationship of heavy metals in soil. The loading  
300 factors of heavy metals elements to the total variance was the main factor in the determination of major pollutants.

301 The first PC (PC1) in component matrix demonstrates that the contamination of Cr originated in the same sources  
302 perhaps, such as waste-water, industrial contamination, lithogenic processes and solid waste. The second PC (PC2)  
303 which consists of Zn and Pb can be defined as anthropogenic components, such as vehicle, industrial fumes which  
304 was a common source of lead contamination in soil (Facchinelli et al., 2001). The high Cd level in the third PC (PC3)  
305 may be related to traffic activities and diesel exhaust. The high scores of PC4 mainly including As and Hg may be  
306 related to the combination of industrial and agricultural activities (Luo et al., 2017). The rotation of the matrix  
307 displayed the same relationship between these heavy metals, which is useful to explain ambiguities in the component  
308 matrix.

### 309 **3.2.2. pollution sources contribution**

310 PMF model was implemented to obtain relevant data to better identify the sources and contributions of heavy  
311 metals in soil (Wang et al., 2019). Five factors were loaded and the percentage of the total number of species was  
312 presented in **Fig. 5b**. **Factor 1** accounted for a high percentage of Hg (56.6%) and Cr (32.7%), the high *CV* of which  
313 reflecting that they may be related to anthropogenic sources (Guan et al., 2018). Such as Hg emissions brought about  
314 by human activities and the emissions caused by waste treatment. On the other hand, Cr can be attributed to emissions  
315 of vehicle activities from the traffic roads (Parra et al., 2014). **Factor 2** was dominated by Pb and Zn, with a percentage  
316 of 44.8% and 55.6%, respectively. It was noted that the concentrations of Pb and Zn were close to the background  
317 values. High concentration distributions of Pb and Zn were mainly concentrated nearby the traffic road, which can  
318 be inferred that the contaminants were from traffic activities or fossil fuel. **Factor 3** explained 40.97% of the total  
319 species to As, which may be caused by utilization of agrochemicals (Xiao et al., 2019). Thus because As was the  
320 main element in the use of pesticides to farmland (Cai et al., 2015). The sharp concentration area of As was around  
321 the sampling site S18 nearby the farmland on the map (Salim et al., 2019). Previous studies had also confirmed that  
322 the enrichment of arsenic was due to the use of pesticides (Liang et al., 2017b). **Factor 4** was defined mainly by Cr  
323 accounting for 45.7% and the accumulation of Cr was mainly associated fine particles from the road area, including

324 atmospheric deposition, coal burning, printing and dyeing industry and metal processing (Wu et al., 2015). Cd  
325 accounted for a large proportion in **factor 5** with the percentage of 44.0%, the main sources of Cd pollution were  
326 lead-zinc mines, smelting of non-ferrous metals, electroplating and factories that use cadmium compounds as raw  
327 materials or catalysts, the same polluted sources as the factor 4 (Wang et al., 2019). The high *CV* value and higher  
328 mean concentration compared with the background value, showing the influence of artificial factor (Gao et al., 2018;  
329 Peng et al., 2017). According to the foregoing investigation, the textile and dyeing industries attributed high content  
330 of Cd from the emission of the sewage of dyeing activities (Wang et al., 2019; Luo et al., 2011; Sun et al., 2019). The  
331 high concentration area and high risk area of metal Cd were all around the dye factory as investigated. Therefore it  
332 was concluded that there were four sources of pollution dominating the contaminated site. Comparatively speaking,  
333 industrial activities occupied the largest contribution to soil heavy metals in the study area; followed by the human  
334 activities such as waste emission. The third largest contribution was made by agricultural activities, which were  
335 related to the farmland in the study area. Owing to the frequent utilization of vehicle and fuel near the roads, traffic  
336 activities accounted for the fourth largest contribution and the followed one was atmospheric deposition. The results  
337 were consistent with the current situation of the whole study area, with abandoned factories, developed transportation  
338 around and frequent agricultural activities, indicating the close relationship between the dye factory and its  
339 surrounding soil.

340 Therefore, the number of factors ought to be set to four within the PMF run by the results of PCA, at that purpose  
341 the simplest analysis results were achieved with a run variety of fifty. Additionally, the coefficients of the six heavy  
342 metal components shown in **Table S3** varied between 0.35 ~ 0.99, indicating that the overall fit of the PMF was  
343 sensible.

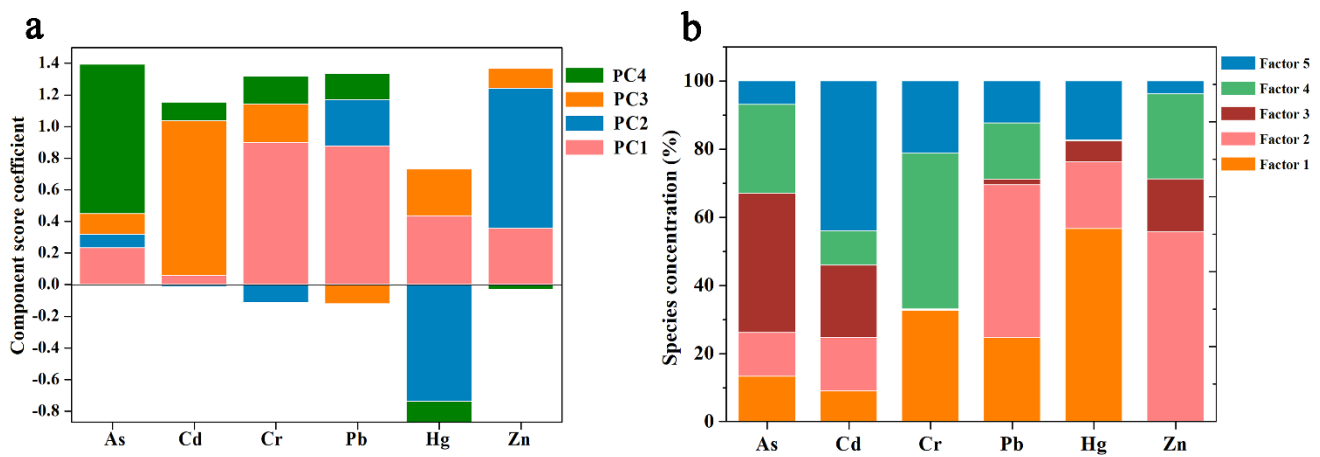


Fig. 5. (a) Component source coefficient by PCA analysis and (b) source contributions for each heavy metal estimated by PMF model.

### 3.3. Human risk assessment

#### 3.3.1. Human risk assessment of heavy metals

The upper limit of 95% confidence intervals of regional survey data ( $C_{95\%}$  UCL in mg/kg) was considered to evaluate of the maximum intake daily dose for human health risk assessment (USEPA, 1989). The original data of *HQ*, *HI* and *THI* (adults and children) by means of classical health risk assessment were presented in **Table 2**. The highest average intake turned out to be the ingestion pathway and the order followed were: dermal contact > inhalation. In the ingestion pathway, average *HQ* ranged as: As > Cd > Pb > Hg > Cr > Zn. *HQs* for six heavy metals were less than 1 both for adults and children, indicating that there were no significant health risks. However, the *THI* value of children through ingestion pathway was 1.00, posing potential health threat to the children. The contribution of As to non-carcinogenic risk was 76.9%, which should be paid attention to in this region. The *CR* values of As, Cd, Cr, Hg, Zn and Pb were evaluated by health risk assessment and the results showed that *CR* index of the whole region for the six heavy metals were all less than 1.0E-06 through ingestion of exposure, indicating that there was no carcinogenic risk in this region. Therefore, the source-contributed assessment of health risks mainly focused on the evaluation of non-carcinogenic health risk. Then the modified assessment of human health risk for five heavy metals was performed based on source contribution (Li et al., 2020).

363 **Table 2**

364 Estimations of human health risk of soil heavy metals.

	Element	Pb	Hg	Cr	Cd	As	Zn	HI	THI
	<i>C-95%</i>	28.75	0.19	71.02	0.76	18.05	68.50		
Adults	<i>HQ<sub>ing</sub></i>	1.13E-02	8.68E-04	4.70E-04	1.20E-02	8.24E-02	3.13E-04	1.07E-01	
	<i>HQ<sub>der</sub></i>	4.46E-05	3.44E-06	1.97E-04	4.79E-05	3.28E-04	1.25E-05	6.33E-04	1.08E-01
	<i>HQ<sub>inh</sub></i>	1.10E-05	6.38E-07	3.46E-06	1.76E-04	2.96E-05	2.30E-07	2.21E-04	
Children	<i>HQ<sub>ing</sub></i>	1.05E-01	8.10E-03	4.39E-03	1.12E-01	7.69E-01	2.92E-03	1.00E+00	
	<i>HQ<sub>der</sub></i>	2.92E-05	2.25E-06	1.29E-04	3.14E-05	2.15E-04	8.16E-06	4.15E-04	1.00E+00
	<i>HQ<sub>inh</sub></i>	1.96E-05	1.14E-06	6.16E-06	3.14E-04	5.26E-05	4.10E-07	3.94E-04	

365 **3.3.2. Source-contributed health risk assessment**

366 The source contribution of *SCCR* and *SCHI* was calculated to evaluate the risk level of the source. The results of  
367 source analysis were incorporated into the health risk model to assess the potential hazards to human health by soil  
368 heavy metals. The calculation of source-contributed health risk assessment could demonstrate the relationship  
369 between pollutants sources and health risk, as shown in **table. 3**. The contributions of the carcinogenic risk assessment  
370 for the heavy metals were demonstrated in **Fig. 6a**. Cr originated from anthropogenic sources, of which Cr accounted  
371 for 5.79E-04. For As, with a high *SCCR* index of 4.50E-04, accounted for the major contributor in the agricultural  
372 activities. For Cr, industrial sources was the main source of pollution in the high *SCCR* area with a *SCCR* index of  
373 1.09E-03. The carcinogenic risk allocation was consistent for adults and children, but the risk values of adults were  
374 lower than that for children. The *TCRs* of the sources were in the order of industry (6.42E-04), agriculture (4.59E-  
375 04), transportation (4.11E-04), and atmosphere (3.23E-04). The industrial sources had the highest *TCR*, indicating  
376 harmful effects from the activities of the dye plant. There was a potential carcinogenic hazard in the study area, for  
377 which reasonable programmes should be developed to reduce or isolate the input or transport of industrial and  
378 agricultural sources. In addition, some activities, particularly industrial and agricultural activities, should be  
379 controlled to reduce population health and environmental risks.

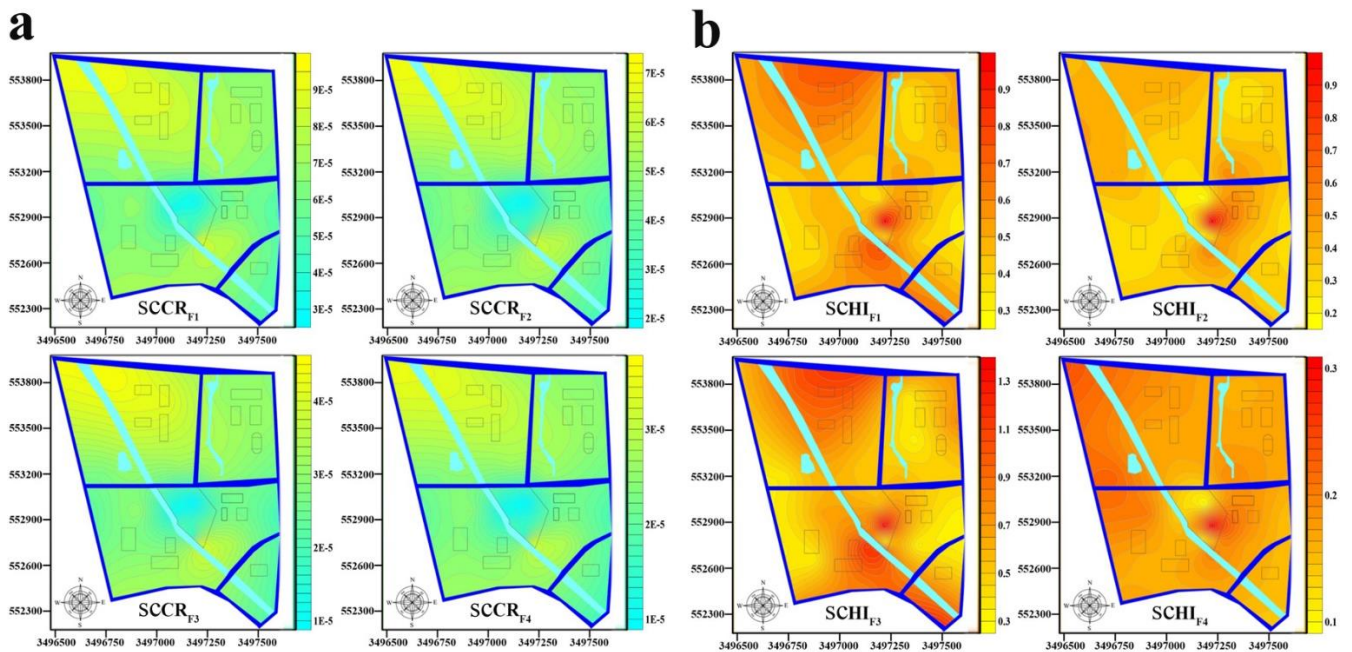
380 The contributions of the non-carcinogenic risk assessment for the heavy metals were demonstrated in **Fig. 6b**. For  
381 Hg and Cr, industrial sources were the main contributors to *SCHI*, accounting for 3.36E-01 and 3.97E-01,

382 respectively. For Pb and Zn, traffic activities was the largest contributor to *SCHI*, accounting for 7.94E-02 and 2.45E-  
 383 02, respectively. For As, the higher *SCHI* came from agricultural activities, with the risk values of 7.96E-02. For Cd,  
 384 *SCHI* was higher from industrial sources at 6.80E-02. The largest contributor to *THI* was industry (6.85E-01),  
 385 followed by traffic sources (4.89E-01), agriculture (4.38E-01), natural (3.44E-01). Industry sources had the highest  
 386 *THI* and were mainly associated with emissions caused by waste treatment of the dye factory, which may contribute  
 387 significant amounts of heavy metals and posed a threat to the local residents.

388 **Table 3**

389 Estimation of non-cancer (hazard index) and cancer risk (total cancer risk) of heavy metals from four sources.

	Children (aged 1-17)					Adults (aged 18+)				
	Factor 1	Factor 2	Factor 3	Factor 4	Total factors	Factor 1	Factor 2	Factor 3	Factor 4	Total factors
	<i>hazard index and total hazard index</i>					<i>hazard index and total hazard index</i>				
As	1.40E-01	1.00E-02	7.96E-02	5.04E-02	4.00E-01	1.51E-03	1.08E-03	9.64E-03	7.-7E-03	4.30E-02
Cd	1.35E-03	9.65E-04	8.65E-04	6.80E-02	3.86E-03	1.47E-04	1.05E-04	9.41E-05	4.40E-02	4.20E-04
Cr	3.97E-01	2.83E-03	2.54E-03	2.00E-02	1.13E+00	5.88E-02	1.20E-04	3.76E-03	2.96E-03	1.68E-01
Hg	3.36E-01	1.40E-02	2.15E-02	1.69E-02	9.59E-02	3.63E-02	2.59E-03	2.32E-03	1.82E-03	1.04E-02
Pb	1.11E-02	7.94E-02	4.11E-02	5.59E-04	3.17E-01	1.20E-02	8.54E-02	7.65E-03	6.01E-03	3.42E-02
Zn	2.03E-03	2.45E-02	1.30E-03	1.02E-03	5.81E-03	2.19E-04	1.56E-02	1.40E-04	1.10E-04	6.25E-04
<b>Total hazard index</b>	6.85E-01	4.89E-01	4.38E-01	3.44E-01	1.96E+00	8.98E-02	6.42E-02	5.75E-02	4.52E-02	2.57E-01
	<i>Cancer risk of each heavy metals and total cancer risk</i>					<i>Cancer risk of each heavy metal and total cancer risk</i>				
As	6.30E-05	4.50E-04	4.03E-06	3.17E-05	3.60E-04	6.82E-06	4.87E-06	4.37E-06	3.43E-06	3.90E-05
Cd	2.38E-10	1.70E-10	1.52E-10	3.20E-04	1.36E-09	1.34E-10	9.55E-11	8.56E-11	6.73E-11	7.64E-10
Cr	1.09E-03	4.13E-05	3.70E-05	2.91E-04	3.31E-03	6.26E-04	4.47E-05	4.01E-05	3.15E-05	3.58E-04
Hg	1.58E-08	1.13E-08	1.01E-08	7.96E-09	9.04E-08	8.89E-09	6.35E-09	5.69E-09	4.47E-09	5.08E-08
<b>Total cancer risks</b>	6.42E-04	4.59E-04	4.11E-04	3.23E-04	3.67E-03	6.95E-05	4.96E-05	4.45E-05	3.49E-05	3.97E-04



390  
391 **Fig. 6.** Spatial distribution of source-contributed carcinogenic and non-carcinogenic risk assessment.

392 **3.4. Discussion of the methodology**

393 To the traditional research, risks assessment under traceability of pollution sources was incorporated into the paper.

394 The evaluation model of the risk allocation of pollution sources was constructed, which was constructive for the

395 treatment of heavy metal soil pollution. It had a certain reference value for the supplement and improvement of the

396 health risk assessment system. The health risk assessment based on source apportionment mainly included optimized

397 spatial interpolation and human health risk. The pollution sources were quantified for health risk assessment, which

398 was optimized compared with conventional risk model. It turned out that the traceability results of the two source-

399 oriented risk assessment model were different as well as the risk contribution order of pollution sources. Source-

400 oriented health risk analysis was at a low risk level, which was dominated by industrial activities. Therefore, Cr

401 should be regarded as the target metal, the emission of which should be converted to hypotoxic elements. It can

402 effectively prevent pollution and realize regional environmental management. Source-oriented human health risk of

403 As was dominated by agricultural activities. So metal arsenic should be treated as a priority target metal for soil

404 pollution. Effective control of metal emission or lowering the concentrations of toxic element can reduce the level of

405 health risk in this region. It was concluded that traditional health risk assessment method may overlook the source

406 contributions of pollution, The traceability and contribution of certain pollution sources combined with health risk  
407 assessment could make up for these deficiencies. In the comparative study of PCA and PMF tracing, it was more  
408 reasonable to take a comprehensive source apportionment for consideration to set definite numbers for pollution  
409 sources. This study provided new insights for the treatment of complex sources and hazards of soil heavy metals.

#### 410 **4. Conclusions**

411 It was of great significance to study the distribution of heavy metal content in abandoned factories and carry out  
412 the comprehensive health risk assessment of heavy metal, so as to provide the basis for the prevention and control of  
413 soil heavy metal pollution. The method was developed by integrating health risk assessment and source contribution  
414 based on source apportionment to study pollutant sources and risk levels. This method optimized spatial interpolation  
415 based on the global content data output so as to quantitatively analyze pollution level of the area intuitively. PCA and  
416 PMF model were carried out by auxiliary quantitative analysis on the determination of pollution sources accurately. A  
417 case study was conducted in an abandoned dye factory in Suzhou City, China, so as to implement the methodology.  
418 This study assessed spatial distribution characteristic and source-identified health risk of six heavy metals (Pb, Hg,  
419 Zn, Cr, Cd, As) in the study area. PMF model was utilized to apportion the sources of risk, combining a receptor  
420 model and a risk model. The source-specific human health risk of heavy metals for each source category was also  
421 discussed, in which some significant results were found. However, owing to anthropogenic influence, the area was  
422 contaminated by these heavy metals studied in some degree. Particularly, industrial activities were identified as the  
423 largest contributor by Cr, mainly associating with the discharge and disposal of pollutants from the dye factory in the  
424 area. The results of source-contributed health risk suggested that there was potential health threat to the children. As  
425 as agriculture activities contributed most to the risk level and would lead to higher risks in the study area. After  
426 comprehensive comparison, it was concluded that in the comparative study after tracing health risks, it was more  
427 reasonable to use comprehensive site risk assessment to treat regional pollution sources in this region. This study  
428 provided a new insight for the treatment of multi-sources of heavy metal and it was advised to reduce the total

429 emission in the process of industry and agriculture by regional structural reconstruction.

#### 430 **Credit authorship contribution statement**

431 Fangfang miao: Data curation, Writing - original draft, Writing –review & editing. Yimei Zhang and Yu Li,  
432 performed the guiding of this paper with support from Yin Zhuang Zhou. Qinglu Fang is mainly responsible for sorting  
433 out data and assisting in drawing. We confirm that this manuscript has not been published elsewhere and is not under  
434 consideration by another journal. We affirm that all authors have approved the submission and the study does not  
435 involve human and animal subjects.

#### 436 **Declaration of Competing Interest**

437 The authors declare that they have no known competing financial interests or personal relationships that could  
438 have appeared to influence the work reported in this paper.

#### 439 **Data availability**

440 The datasets generated and analyzed during the current study are not publicly available due to its confidentiality  
441 but are available from the corresponding author on reasonable request.

#### 442 **Acknowledgments**

443 This work was financially supported by the National Key R&D Program of China (No. 2018YFB0605504) and  
444 the National Natural Science Foundation of China (Grant No. 51878272). This work was supported by MOE Key  
445 Laboratory of Resources and Environmental Systems Optimization (NCEPU). The authors also would like to express  
446 their heartfelt gratitude to the support of National University of Singapore Suzhou research institute. Sincere gratitude  
447 should be expressed to the editors and reviewers who have put considerable time and efforts into their comments on  
448 this paper.

#### 449 **References**

450 Adimalla, N., Qian, H., Wang, H.K., 2019. Assessment of heavy metal (HM) contamination in agricultural soil lands in northern  
451 Telangana, India: an approach of spatial distribution and multivariate statistical analysis. *Environ.Monit. Assess.* 191, 246.  
452 <https://doi.org/10.1007/s10661-019-7408-1>.

453 Bryanin, S.V., Sorokina, O.A., 2019. Effect of soil properties and environmental factors on chemical compositions of forest soils in the  
454 Russian Far East. *J. Soils Sediments* 19, 1130-1138. <https://doi.org/10.1007/s11368-018-2141-x>.

455 Cai, L., Xu, Z., Bao, P., He, M., Dou, L., Chen, L., Zhou, Y., Zhu, Y.G., 2015. Multivariate and geostatistical analyses of the spatial  
456 distribution and source of arsenic and heavy metals in the agricultural soils in Shunde, Southeast China. *J. Geochem.Explor.* 148,  
457 189-195. <https://doi.org/10.1016/j.gexplo.2014.09.010>.

458 Chen, H., Teng, Y., Lu, S., Wang, Y., Wang, J., 2015. Contamination features and health risk of soil heavy metals in China. *Sci. Total*  
459 *Environ.* 512, 143–153. <https://doi.org/10.1016/j.scitotenv.2015.01.025>.

460 Chen, J.Q., Wang, Z.X., Wu, X., Zhu, J.J., Zhou, W.B., 2011. Source and hazard identification of heavy metals in soils of Changsha based  
461 on TIN model and direct exposure method. *Trans. Nonferrous Metals Soc. China* 21 (3), 642-651. [https://doi.org/10.1016/S1003-](https://doi.org/10.1016/S1003-6326(11)60761-9)  
462 [6326\(11\)60761-9](https://doi.org/10.1016/S1003-6326(11)60761-9).

463 Cheng, S., Liu, G., Zhou, C., Sun R., 2018. Chemical speciation and risk assessment of cadmium in soils around a typical coal mining  
464 area of China. *Ecotox. Environ. Safe.* 160, 67-74. <https://doi.org/10.1016/j.ecoenv.2018.05.022>.

465 CNEPA (National Environment Protection Agency of China), 1995, Environment Quality Standard for Soils (GB 15618-1995) (in  
466 Chinese).

467 CSC (China State Council), 2016. The action plan for soil pollution prevention and control. Available at:  
468 [http://www.gov.cn/zhengce/content/2016-05/31/content\\_5078377.htm](http://www.gov.cn/zhengce/content/2016-05/31/content_5078377.htm) (accessed in November) (in Chinese).

469 De Miranda, R.M., de Fatima Andrade, M., Dutra Ribeiro, F.N., Mendonça Francisco, K.J., Pérez-Martínez, P.J., 2018, Source  
470 apportionment of fine particulate matter by positive matrix factorization in the metropolitan area of São Paulo, Brazil. *J. Clean Prod.*  
471 202, 253–263. <https://doi.org/10.1016/j.jclepro.2018.08.100>.

472 Dong, R.Z., Jia, Z.M., Li, S.Y., 2018. Risk assessment and sources identification of soil heavy metals in a typical county of Chongqing  
473 municipality, Southwest China. *Process Saf. Environ. Prot.* 113, 275-281. <https://doi.org/10.1016/j.psep.2017.10.021>.

474 Duan, J.C., Tan, J.H., Hao, J.M., Chai, F.H., 2014. Size distribution, characteristics and sources of heavy metals in haze episod in Beijing.  
475 *J. Environ. Sci.* 26, 189-196. [https://doi.org/10.1016/S1001-0742\(13\)60397-6](https://doi.org/10.1016/S1001-0742(13)60397-6).

476 Duan, Y.X., Zhang, Y.M., Li, S., Fang, Q.L., Miao, F.F., Lin, Q.G., 2020, An integrated method of health risk assessment based on spatial  
477 interpolation and source apportionment. *J. Clean Prod.* 276. <https://doi.org/10.1016/j.jclepro.2020.123218>.

478 Franco-Uría, A., López-Mateo, C., Roca, E., Fernández-Marcos, M.L., 2009. Source identification of heavy metals in pastureland by  
479 multivariate analysis in NW Spain. *J. Hazard. Mater.* 165, 1008-1015. <https://doi.org/10.1016/j.jhazmat.2008.10.118>.

480 Fu, W.J., Jiang, P.K., Zhou, G.M., Zhao, K.L., 2014. Using Moran's I and GIS to study the spatial pattern of forest litter carbon density in  
481 a subtropical region of southeastern China. *Biogeosciences.* 11, 2401-2409. <https://doi.org/10.5194/bg-11-2401-2014>.

482 Gao, J., Wang, L.C., 2018. Ecological and human health risk assessments in the context of soil heavy metal pollution in a typical industrial  
483 area of Shanghai, China. *Environ. Sci. Pollut. Res.* 25, 27090-27105. <https://doi.org/10.1007/s11356-018-2705-8>.

484 Gholizadeh, A., Taghavi, M., Moslem, A., Neshat, A.A., Lari Najafi, M., Alahabadi, A., Ahmadi, E., Ebrahimi Aval, H., Asour, A.A.,  
485 Rezaei, H., Gholami, S., Miri, M., 2019. Ecological and health risk assessment of exposure to atmospheric heavy metals. *Ecotoxicol.*  
486 *Environ. Saf.* 184, 109622. <https://doi.org/10.1016/j.ecoenv.2019.109622>.

487 Goix, S., Resongles, E., Point, D., Oliva, P., Duprey, J.L., de la Galvez, E., Ugarte, L., Huayta, C., Prunier, J., Zouiten, C., Gardon, J.,  
488 2013. Transplantation of epiphytic bioaccumulators (*Tillandsia capillaris*) for high spatial resolution biomonitoring of trace elements  
489 and point sources deconvolution in a complex mining/smelting urban context. *Atmos. Environ.* 80, 330 - 341.

490 Guan, Q., Wang, F., Xu, C., Pan, N., Lin, J., Zhao, R., 2018. Source apportionment of heavy metals in agricultural soil based on PMF: A  
491 case study in Hexi Corridor, northwest China. *Chemosphere* 193, 189-197. <https://doi.org/10.1016/j.chemosphere.2017.10.151>.

492 Guo, G., Wu, F., Xie, F., Zhang, R., 2012. Spatial distribution and pollution assessment of heavy metals in urban soils from southwest  
493 China. *J Environ Sci.* 24,410-418. [https://doi.org/10.1016/S1001-0742\(11\)60762-6](https://doi.org/10.1016/S1001-0742(11)60762-6).

494 Hakanson, L., Håkanson, L., Hakansson, L., 1980. An ecological risk index for aquatic pollution control: a sediment ecological approach.  
495 *Water Res.* 14, 975-1001. [https://doi.org/10.1016/0043-1354\(80\)90143-8](https://doi.org/10.1016/0043-1354(80)90143-8).

496 Han, Y., Du, P., Cao, J., Posmentier, E.S., 2006. Multivariate analysis of heavy metal contamination in urban dusts of Xi'an, Central  
497 China. *Sci. Total Environ.* 355, 176-186. <https://doi.org/10.1016/j.scitotenv.2005.02.026>.

498 Hu, W., Wang, H., Dong, L., Borggaard, O.K., Hansen, H.C.B., He, Y., Holm, P.E., 2018. Source identification of heavy metals in peri-  
499 urban agricultural soils of southeast China: an integrated approach. *Environ. Pollut.* 237, 650-661.  
500 <https://doi.org/10.1016/j.envpol.2018.02.070>.

501 Huang, B., Shi, X.Z., Yu, D.S., Oborn, I., Blomback, K., Pagella, T.F., Wang, H.J., Sun, W.X., Sinclair, F.L., 2006. Environmental  
502 assessment of small-scale vegetable farming systems in peri-urban areas of the Yangtze River Delta Region, China. *Agric. Ecosyst.*  
503 *Environ.* 112, 391-402. <https://doi.org/10.1016/j.agee.2005.08.037>.

504 Ihedioha, J.N., Ukoha, P.O., Ekere, N.R., 2017. Ecological and human health risk assessment of heavy metal contamination in soil of a  
505 municipal solid waste dump in Uyo, Nigeria. *Environ. Geochem. Health* 39, 497-515. <https://doi.org/10.1007/s10653-016-9830-4>.

506 Islam, S., Ahmed, K., Mamun, H.A., Eaton, D.W., 2017. Human and ecological risks of metals in soils under different land use in an  
507 urban environment of Bangladesh. *Pedosphere*, S1002016017603953. [https://doi.org/10.1016/S1002-0160\(17\)60395-3](https://doi.org/10.1016/S1002-0160(17)60395-3).

508 Järup, L., 2003, Hazards of heavy metal contamination, *Br. Med. Bull.* 68, 167-182. <https://doi.org/10.1093/bmb/ldg032>.

509 Jia, J., Li, X., Wu, P., Liu, Y., Han, C., Zhou, L., Yang, L., 2015. Human health risk assessment and safety threshold of harmful trace  
510 elements in the soil environment of the wulantuga open-cast coal mine, *Minerals* 5, 0528.  
511 <https://doi.org/info:doi/10.3390/min5040528>.

512 Jiang, F., Ren, B.Z., Hursthouse, A., Deng, R.J., Wang, Z.H., 2019. Distribution, source identification, and ecological-health risks of  
513 potentially toxic elements (PTEs) in soil of thallium mine area (southwestern Guizhou, China). *Environ. Sci. Pollut. Res.* 26, 16556-  
514 16567. <https://doi.org/10.1007/s11356-019-04997-3>.

515 Jiang, H., Cai, L., Wen, H., Hu, G., Chen, L., Luo, J., 2019. An integrated approach to quantifying ecological and human health risks  
516 from different sources of soil heavy metals. *Sci. Total Environ.* 134466 <https://doi.org/10.1016/j.scitotenv.2019.134466>.

517 Kumar, V., Sharma, A., Kaur, P., Sidhu, GPS., Bali, AS., Bhardwaj, R., 2019. Pollution assessment of heavy metals in soils of India and  
518 ecological risk assessment: A state-of-the-art. *Chemosphere* 216, 449-462. <https://doi.org/10.1016/j.chemosphere.2018.10.066>.

519 Kurt-Karakus P B K. 2012. Determination of heavy metals in indoor dust from Istanbul, Turkey: Estimation of the health risk. *Environ*  
520 *Int.* 50, 47–55. <https://doi.org/10.1016/j.envint.2012.09.011>.

521 Larsen, R.K., Baker, J.E., 2003, Source apportionment of polycyclic aromatic hydrocarbons in the urban atmosphere: a comparison of  
522 three methods. *Environ. Sci. Technol.* 37, 1873-1881. <https://doi.org/10.1021/es0206184>.

523 Li, P., Xue, R., Wang, Y., Zhang, R., Zhang, G., 2015. Influence of anthropogenic activities on PAHs in sediments in a significant gulf  
524 of low-latitude developing regions, the Beibu Gulf, South China Sea: distribution, sources, inventory and probability risk. *Mar.*  
525 *Pollut. Bull.* 90 (1 – 2), 218 – 226.

526 Li, Y., Chen, H., Teng, Y., 2020. Source apportionment and source-oriented risk assessment of heavy metals in the sediments of an urban  
527 river-lake system. *Sci. Total Environ.* 140310. <https://doi.org/10.1016/j.scitotenv.2020.140310>.

528 Liang, J., Feng, C., Zeng, G., Gao, X., Zhong, M., Li, X., 2017a. Spatial distribution and source identification of heavy metals in surface  
529 soils in a typical coal mine city, Lianyuan, China. *Environ. Pollut.* 225, 681-690. <https://doi.org/10.1016/j.envpol.2017.03.057>.

530 Liang, J., Feng, C., Zeng, G., Gao, X., Zhong, M., Li, X., He, X., Fang, Y., 2017b. Spatial distribution and source identification of heavy  
531 metals in surface soils in a typical coal mine city, Lianyuan, China. *Environ Pollut.* 225, 681-690. [https://doi.o](https://doi.org/10.1016/j.envpol.2017.03.057)  
532 [rg/10.1016/j.envpol.2017.03.057](https://doi.org/10.1016/j.envpol.2017.03.057).

533 Liu, B., Ai, S., Zhang, W., Huang, D., Zhang, Y., 2017. Assessment of the bioavailability, bioaccessibility and transfer of heavy metals  
534 in the soil-grain-human systems near a mining and smelting area in NW China. *Sci. Total Environ.* 609, 822–829. [https://doi.org/](https://doi.org/10.1016/j.scitotenv.2017.07.215)  
535 [10.1016/j.scitotenv.2017.07.215](https://doi.org/10.1016/j.scitotenv.2017.07.215).

536 Liu, X., Ying, L., Lu, S., 2018, Occurrence of typical antibiotics and source analysis based on PCA-MLR method in the East Dongting  
537 Lake, China. *Ecotox. Environ. Safe.* 163, 145-152. <https://doi.org/10.1016/j.ecoenv.2018.07.067>.

538 Luo, C., Liu C., Wang, Y., Liu, X., Li, F., Zhang, G., 2011. Heavy metal contamination in soils and vegetables near an e-waste processing  
539 site, South China. *J Hazard Mater.* 186, 481-90. <https://doi.org/10.1016/j.jhazmat.2010.11.024>.

540 Luo, X., Xue, Y., Wang, Y., Cang, L., Xu, B., Ding, J., 2015. Source identification and apportionment of heavy metals in urban soil  
541 profiles. *Chemosphere.* 127, 152–157. <https://doi.org/10.1016/j.chemosphere.2015.01.048>.

542 Luo X S, Yu S, Li X D. 2011. Distribution, availability, and sources of trace metals in different particle size fractions of urban soils in  
543 Hong Kong: Implications for assessing the risk to human health. *Environ Pollut.* 159, 1317–1326. [https://doi.org/  
544 10.1016/j.envpol.2011.01.013](https://doi.org/10.1016/j.envpol.2011.01.013).

545 Lv, J., Liu, Y., 2019. An integrated approach to identify quantitative sources and hazardous areas of heavy metals in soils. *Sci. Total*  
546 *Environ.* 646, 19–28. <https://doi.org/10.1016/j.scitotenv.2018.07.257>.

547 Lv, J.S., 2019. Multivariate receptor models and robust geostatistics to estimate source apportionment of heavy metals in soils. *Environ.*  
548 *Pollut.* 244, 72-83. <https://doi.org/10.1016/j.scitotenv.2005.02.026>.

549 Ma, Z., Chen, K., Li, Z., Bi, J., Huang, L., 2015. Heavy metals in soils and road dusts in the mining areas of Western Suzhou, China: a  
550 preliminary identification of contaminated sites. *J SOIL SEDIMENT* 16, 204-214. <https://doi.org/10.1007/s11368-015-1208-1>.

551 Mamut, A., Eziz, M., Mohammad, A., Anayit, M., 2017. The spatial distribution, contamination, and ecological risk assessment of heavy  
552 metals of farmland soils in Karashahar-Baghrash oasis, northwest China. *Hum. Ecol. Risk Assess.* 23, 1300-1314.  
553 <https://doi.org/info:doi/10.1080/10807039.2017.1305263>.

554 Mao, C., Song, Y., Chen, L., Ji, J., Li, J., Yuan, X., Yang, Z., Ayoko, G.A., Frost, R.L., Theiss, F.L., 2019. Human health risks of heavy  
555 metals in paddy rice based on transfer characteristics of heavy metals from soil to rice. *Catena* 175, 339–348.  
556 <https://doi.org/10.1016/j.catena.2018.12.029>.

557 Mendoza, C.J., Garrido, R.T., Quilodr an, R.C., Segovia, C.M., Parada, A.J., 2017. Evaluation of the bioaccessible gastric and intestinal  
558 fractions of heavy metals in contaminated soils by means of a simple bioaccessibility extraction test. *Chemosphere* 176, 81–88.  
559 <https://doi.org/10.1016/j.chemosphere.2017.02.066>.

560 Mohammadi, A.A., Zarei, A., Esmacilzadeh, M., Taghavi, M., Yousefi, M., Yousefi, Z., Sedighi, F., Javan, S., 2020. Assessment of heavy  
561 metal pollution and human health risks assessment in soils around an industrial zone in Neyshabur, Iran. *Biol. Trace Elem. Res.*  
562 195, 343–352. <https://doi.org/10.1007/s12011-019-01816-1>.

563 National Environmental Protection Agency (NEPA), 1995. Environmental Quality Standard for Soils (GB 15618-1995). National  
564 Environmental Protection Agency of China, Beijing.

565 Nazzal, Y., Howari, FM., Jafri, MK., Naeem, M., Ghrefat, H., 2016. Risk assessment through evaluation of potentially toxic metals in  
566 the surface soils of the Qassim area, Central Saudi Arabia. *Ital. J. Geosci.* 135, 210-216. <https://doi.org/10.3301/IJG.2015.10>.

567 Noll, M.R., 2002. Trace elements in terrestrial environments: biogeochemistry, bioavailability, and risks of metals. *J. Environ. Qual.* 32,  
568 374. <https://doi.org/10.2134/jeq2002.3740>.

569 Norris, G., Duvall, R., Brown, S., Bai, S., 2014. EPA Positive Matrix Factorization (PMF) 5.0 Fundamentals and User Guide. US  
570 Environmental Protection Agency, Washington, DC.

571 Ouyang, Z., Gao, L., Yang, C., 2018. Distribution, sources and influence factors of polycyclic aromatic hydrocarbon at different depths  
572 of the soil and sediments of two typical coal mining subsidence areas in Huainan, China. *Ecotox. Environ. Safe.* 163, 255-265.  
573 <https://doi.org/10.1016/j.ecoenv.2018.07.024>.

574 Paatero, P., Tapper, U., 1994. Positive matrix factorization: a non-negative factor model with optimal utilization of error estimates of  
575 data values. *Environmetrics* 5, 111-126. [CCC 1 180-4009/94/020 1 1 1 – 16](https://doi.org/10.1002/env.111).

576 Papa S, Bartoli G, Pellegrino A, Fioretto A. 2010. Microbial activities and trace element contents in an urban soil. *Environ Monit Assess.*  
577 165, 193–203. [https://doi.org/ 10.1007/s10661-009-0938-1](https://doi.org/10.1007/s10661-009-0938-1).

578 Parra, S., Bravo, M.A., Quiroz, W., Moreno, T., Karanasiou, A., Font, O., Vidal, V., Cereceda-Balic, F., 2014. Source apportionment for  
579 contaminated soils using multivariate statistical methods. *Chemom. Intell. Lab. Syst.* 138, 127-132. [https://doi.org/  
580 10.1016/j.chemolab.2014.08.003](https://doi.org/10.1016/j.chemolab.2014.08.003).

581 Peng, X., Shi, G.L., Liu, G.R., Xu, J., Tian, Y.Z., Zhang, Y.F., Feng, Y.C., Russell, A.G., 2017, Source apportionment and heavy metal  
582 health risk (HMHR) quantification from sources in a southern city in China, using an ME2-HMHR method. *Environ. Pollut.* 221,  
583 335-342. <https://doi.org/10.1016/j.envpol.2016.11.083>.

584 Salim, I., Sajjad, R.U., Paule-Mercado, M.C., Memon, S.A., Lee, B.Y., Sukhbaatar C., 2019. Comparison of two receptor models PCA-  
585 MLR and PMF for source identification and apportionment of pollution carried by runoff from catchment and sub-watershed areas  
586 with mixed land cover in South Korea. *Sci Total Environ.* 663, 764-775. <https://doi.org/10.1016/j.scitotenv.2019.01.377>.

587 Salmani-Ghabeshi, S., Palomo-Marin, M.R., Bernalte, E., Rueda-Holgado, F., Miró-Rodríguez, C., Cereceda-Balic, F., Fadic, X., Vidal,  
588 V., Funes, M., Pinilla-Gil, E., 2016, Spatial gradient of human health risk from exposure to trace elements and radioactive pollutants  
589 in soils at the Puchuncaví-Ventanas industrial complex, Chile. *Environ. Pollut.* 218, 322-330.  
590 <https://doi.org/10.1016/j.envpol.2016.07.007>.

591 Sun, L., Guo, D.K., Liu, K., Meng, H., Zheng, Y.J., Yuan, F.Q., Zhu, G.H., 2019. Levels, sources, and spatial distribution of heavy metals  
592 in soils from a typical coal industrial city of Tangshan, China. *Catena* 175, 101-109. <https://doi.org/10.1016/j.catena.2018.12.014>.

593 Tapia-Gatica, J., Gonzalez-Miranda, I., Salgado, E., Bravo, M.A., Tessini, C., Dovletyarova, E.A., Paltseva, A.A., Neaman, A., 2020.  
594 Advanced determination of the spatial gradient of human health risk and ecological risk from exposure to As, Cu, Pb, and Zn in  
595 soils near the Ventanas Industrial Complex (Puchuncaví, Chile). *Environ. Pollut.* 258, 113488.  
596 <https://doi.org/10.1016/j.envpol.2019.113488>.

597 Teng, Y., Ni, S., Wang, J., Zuo, R., Yang, J., 2010. A geochemical survey of trace elements in agricultural and non-agricultural topsoil  
598 in Dexing area, China. *Journal of Geochemical Exploration* 104, 118–127.

599 Tian, K., Huang, B., Xing, Z., Hu, W., 2017. Geochemical baseline establishment and ecological risk evaluation of heavy metals in  
600 greenhouse soils from Dongtai, China. *Ecol. Indic.* 72, 510-520. <https://doi.org/10.1016/j.ecolind.2016.08.037>.

601 Tian, S., Liang, T., Li, K., Wang, L., 2018, Source and path identification of metals pollution in a mining area by PMF and rare earth  
602 element patterns in road dust. *Sci. Total. Environ.* 633, 958-966. <https://doi.org/10.1016/j.scitotenv.2018.03.227>.

603 USEPA (United States Environmental Protection Agency), 2014. EPA positive matrix factorization (PMF) 5.0 fundamentals and user  
604 guide. In: Norris, G., Duvall, R., Brown, S., Bai, S. (Eds.), EPA/600/R-14/108 (NTIS PB2015-105147), Washington, DC.

605 Wang, S., Cai, L.M., Wen, H.H., Luo, J., Wang, Q.S., Liu, X., 2018. Spatial distribution and source apportionment of heavy metals in  
606 soil from a typical county-level city of Guangdong Province, China. *Sci Total Environ.* 655, 92-101. [https://doi.org/  
607 10.1016/j.scitotenv.2018.11.244](https://doi.org/10.1016/j.scitotenv.2018.11.244).

608 Wang, S., Cai, L., Wen, H., Luo, J., Wang, Q., Liu, X., 2019a. Spatial distribution and source apportionment of heavy metals in soil  
609 from a typical county-level city of Guangdong Province, China. *Sci. Total. Environ.* 655, 92-101.  
610 <https://doi.org/10.1016/j.scitotenv.2018.11.244>.

611 Wang, S., Hu, G., Yan, Y., Wang, S., Yu, R., Cui, J., 2019b, Source apportionment of metal elements in PM2.5 in a coastal city in  
612 Southeast China: Combined Pb-Sr-Nd isotopes with PMF method. *Atmos. Environ.* 198, 302-312.  
613 <https://doi.org/10.1016/j.atmosenv.2018.10.056>.

614 Wcisło, E., Bronder, J., Bubak, A., Rodríguez-Valdés, E., Gallego, J.L.R., 2016. Human health risk assessment in restoring safe and  
615 productive use of abandoned contaminated sites, *Environ. Int.* 94, 436–448. <https://doi.org/10.1016/j.envint.2016.05.028>.

616 Wu, Q., Leung, JYS., Geng, X., Chen, S., Huang, X., Li, H., 2015. Heavy metal contamination of soil and water in the vicinity of an  
617 abandoned e-waste recycling site: Implications for dissemination of heavy metals. *Sci Total Environ.* 506, 217-225. [https://doi.org/  
618 10.1016/j.scitotenv.2014.10.121](https://doi.org/10.1016/j.scitotenv.2014.10.121).

619 Wu, W., Dong, C., Wu, J., Liu, X., Wu, Y., Chen, X., Yu, S., 2017. Ecological effects of soil properties and metal concentrations on the  
620 composition and diversity of microbial communities associated with land use patterns in an electronic waste recycling region. *Sci.*  
621 *Total Environ.* 601, 57-65. <https://doi.org/10.1016/j.scitotenv.2017.05.165>.

622 Xiao-Bo, N., X. Wen-Hua, F. Xi, Y. Wen-De, and D. Xiang-Wen, 2009, Heavy metal concentrations and pollution assessment of  
623 limestone forests in Huaxi district, Guiyang City: *Acta Ecologica Sinica*, v. 29, 2169-2177.

624 Xiao, R., Guo, D., Ali, A., Mi, S., Liu, T., Ren, C., Li, R., Zhang, Z., 2019. Accumulation, ecological-health risks assessment, and source  
625 apportionment of heavy metals in paddy soils: A case study in Hanzhong, Shaanxi, China. *Environ. Prot.* 248, 349-357.  
626 [https://doi.org/ 10.1016/j.envpol.2019.02.045](https://doi.org/10.1016/j.envpol.2019.02.045).

627 Xie, Z., Xiang, L., Du, Z., Jiang, Y., Zhang, H., Wu, Y., Long, T., 2016. Accumulation of heavy metals in a coastal wetland natural reserve  
628 in the estuarine wetlands of Tianjin, China. In: 2016 International Congress on Computation Algorithms in Engineering (Iccae  
629 2016), pp. 271-280.

630 Xue, J., Y. Zhi, L. Yang, J. Shi, L. Zeng, and L. Wu, 2014, Positive matrix factorization as source apportionment of soil lead and cadmium  
631 around a battery plant (Changxing County, China): *ENVIRON SCI POLLUT R.* 21, 7698-7707.

632 Zhang, H., Wan, Z., Ding, M., 2018. Inherent bacterial community response to multiple heavy metals in sediment from river-lake systems  
633 in the Poyang Lake, China. *Ecotox. Environ. Safe* 165, 314–324. <https://doi.org/10.1016/j.ecoenv.2018.09.010>.

634 Zhang, Y., Wang, F., Zhang, D., Chen, J., Zhu, H., Zhou, L., Chen, Z., 2017. New type multifunction porous aerogels for supercapacitors  
635 and absorbents based on cellulose nanofibers and graphene, *Mater. Lett.* 208 ,73–76. <https://doi.org/10.1016/j.matlet.2017.04.141>.

636 Zhang, Y., Yin, C., Cao, S., Cheng, L., Wu, G., Guo, J., 2018a, Heavy metal accumulation and health risk assessment in soil-wheat

637 system under different nitrogen levels. *Sci. Total. Environ.* 622-623, 1499-1508. <https://doi.org/10.1016/j.scitotenv.2017.09.317>.

638 Zhang, Y., Zhang, D., Zhou, L., Zhao, Y., Chen, J., Chen, Z., Wang, F., 2018b. Polypyrrole/ reduced graphene oxide aerogel particle  
639 electrodes for high-efficiency electro-catalytic synergistic removal of Cr(VI) and bisphenol A, *Chem. Eng. J.* 336, 690–700.  
640 <https://doi.org/10.1016/j.cej.2017.11.109>.

641 Zhao, L., Xu, Y., Hou, H., Shangguan, Y., Li, F., 2014. Source identification and health risk assessment of metals in urban soils around  
642 the Tanggu chemical industrial district, Tianjin, China. *Sci. Total Environ.* 468, 654-662.  
643 <https://doi.org/10.1016/j.scitotenv.2013.08.094>.

644 Zhou, J., and Z. Sha, 2013, A New Spatial Interpolation Approach Based on Inverse Distance Weighting: Case Study from Interpolating  
645 Soil Properties, *Communications in Computer & Information Science*, 399, 623-631.

646 Zhu, H.N., Yuan, X.Z., Zeng, G.M., Jiang, M., Liang, J., Zhang, C., 2012. Ecological risk assessment of heavy metals in sediments of  
647 Xiawan port based on modified potential ecological risk index. *Trans. Nonferrous Metals Soc. China* 22, 1470-1477.  
648 [https://doi.org/10.1016/S1003-6326\(11\)61343-5](https://doi.org/10.1016/S1003-6326(11)61343-5).

## Supplementary Files

This is a list of supplementary files associated with this preprint. Click to download.

- [SupplementaryMaterial.docx](#)